

Quantum Circuits for maximally entangled states

Alba Cervera-Lierta,^{1,2} José Ignacio Latorre,^{2,3,4} and Dardo Goyeneche⁵

¹*Barcelona Supercomputing Center (BSC)*

²*Dept. Física Quàntica i Astrofísica, Universitat de Barcelona, Barcelona, Spain.*

³*Nikhef Theory Group, Science Park 105, 1098 XG Amsterdam, The Netherlands.*

⁴*Center for Quantum Technologies, National University of Singapore, Singapore.*

⁵*Departamento de Física, Facultad de Ciencias Básicas,
Universidad de Antofagasta, Casilla 170, Antofagasta, Chile*

(Dated: April 18, 2019)

We design a series of quantum circuits that generate absolute maximally entangled (AME) states to benchmark a quantum computer. A relation between graph states and AME states can be exploited to optimize the structure of the circuits and minimize their depth. Furthermore, we find that most of the provided circuits obey majorization relations for every partition of the system, and at every step of the quantum computation. The rationale for our approach is to benchmark quantum computers with maximal useful entanglement, which can be used to implement multipartite quantum protocols.

Keywords: Absolutely maximally entanglement, quantum computing, quantum circuits.

I. INTRODUCTION

There is a need to set up a thorough benchmarking strategy for quantum computers. Devices that operate in very different platforms are often characterized by the number of qubits they offer, their coherent time and the fidelities of one- and two-qubit gates. This is somewhat misleading as the performance of circuits are far below the expected accuracy if errors of gates were to be taken at face value and considered independent.

There exist several figures of merit that try to quantify the success performance of a quantum device. Methods such as randomized benchmarking [1], state and process tomography [2] and gateset tomography [3, 4] are used to quantify gate fidelities. However, they are only useful for few-qubit experiments and fail when used to evaluate the performance of greater circuits [5, 6]. In that sense, IBM proposed a metric to be used in arbitrary large quantum circuits called *quantum volume* [7]. This figure takes into account several circuit variables like number of qubits, connectivity and gate fidelities. The core of the protocol is the construction of arbitrary circuits formed by one- and two-qubit gates that are complex enough to reproduce a generic n -qubit operation. One can expect to generate high entanglement in this kind of circuits. Even though, we should certify that this amount of entanglement will be large enough to perform some specific tasks that, precisely, demand high entanglement. A further relevant reference concerns to volumetric framework for quantum computer benchmarks [8].

A reasonable test for a quantum computer may be based on the construction of maximally entangled states, or the solution of certain hard problems via quantum circuits. The rationale for the former proposal is clear. Quantum advantage will need quantum computers to be able to handle very large entanglement, to make classical computers unable to carry the demanded task even if techniques such as tensor networks are used [9]. As for the second way of testing quantum computers on complete circuits solving difficult problems there is little doubt that it makes sense. For instance, a quantum computer factoring large numbers would be considered successful. Although present quantum computers may be still far from solving difficult tasks, they are definitely ready to be tested on highly entangled states.

Following this line of thought, we shall here explore the construction of highly entangled states using prescribed quantum circuits that we shall present. Some previous results that pathed the way are known. For instance, it was observed that the desired violation of Bell inequalities on a quantum computer deteriorates as the number of qubits increase, although the number of gates needed is not very large [10]. Another example is the exact simulation in a quantum computer of an analytical solvable model. The results obtained from several quantum computers differ significantly from the expected values, even for a small experiment involving four qubits and less than thirty basic quantum gates [11]. These examples illustrate the difference between gate fidelity and circuit fidelity. The second is far more difficult to attain. Quantum correlations depend on the delicate balance of the coefficients of the wave function. It is natural to expect that quantum computers will have to be very refined to achieve such a good description of multipartite correlations along the successive action of gates. Entanglement is at the heart of quantum efficiency [12]. Again, if a quantum computer is not able to generate faithful large entanglement, it will remain inefficient.

It is natural to try to put stress into a quantum computer by demanding that it should not only be able to generate large entangled states (such as area law violating states) but that it should support controlled maximal entanglement.

To be precise, a quantum computer should not only be able to deal with GHZ-like states, as needed to violate qubit Bell inequalities [13], but should allow for the construction of Absolute Maximally Entangled (AME) states [14–16], which are maximally entangled in every partition of the system. The latter requirement is more stringent, as all reduced density matrices should be of maximal rank, as opposed e.g. to rank two in the case of GHZ states.

In the following, we shall present the circuits that are necessary to build the most entangled states under full control. This proposal is distinctly different from bosonic sampling, where large entanglement is developed along the circuit to make it impossible to be faithfully reproduced by classical simulation [17]. For AME states are well understood and serve to fulfill genuine advanced quantum protocols, such as multipartite teleportation [18] or quantum secret sharing [16, 18]. In a sense, maximally entangled states are a test for a useful quantum computer, not for quantum advantage.

The present manuscript details a benchmark suit of quantum circuits, where each one should deliver an AME state. The circuits provided have been designed to minimize the number of required gates. Some of them deal with qudits of different dimensions and are reduced to qubits on specific examples. In general, we have seek for simple and compact circuits. As much as possible, we have also connected the construction of AME state to graphs that illustrate the way entanglement is generate at every step of the circuit. We have also paid attention to the idea of majorization, that is, whether entanglement follows a fine tuned increase for all partitions such that all eigenvalues of the reduced density matrices obey majorization relations.

This work is structured as follows. First, in section II, we review the basic properties of AME states and the explicit structure of some examples. Next, in section III, we present the quantum circuits that generates these states by using the properties of graph states. We also propose the simulation of AME states of dimension greater than 2 using qubits instead of qudits. Finally, in section IV, we analyze the entanglement majorization in the circuits proposed and we find more optimal circuits for the experimental implementation by imposing a majorization arrow in terms of entanglement. The conclusions of this test for a quantum computer are exposed in section VI.

II. REVIEW OF AME STATES

The study of AME states have become an intensive area of research along the last years due to both theoretical foundations and practical applications. In this section we briefly review the current state of the art of the field. For a more extensive review on AME states, see e.g. Ref. [15].

A. General properties of AME states

AME states, also known in some references as *maximally multipartite entangled states*, are n qudit quantum states with local dimension d such that every reduction to $\lfloor n/2 \rfloor$ parties is maximally mixed. Such states are maximally entangled when considering the entropy of reductions as a measure of multipartite entanglement, that is, the average entropy of these states is $S = \lfloor n/2 \rfloor$, when taking logarithm in basis d .

The existence of AME states for n qudit systems, denoted as $\text{AME}(n, d)$, is a hard open problem [19]. Only for the case of qubit systems, i.e. $d = 2$, the problem is fully solved for any n : an $\text{AME}(n, 2)$ exists only for $n = 2, 3, 5, 6$. [20–23]. For instance, Bell states and GHZ states are AME for bipartite and three partite systems of any d , respectively.

Among all existing AME states, there is one special class composed by minimal support states. These state are defined as follows: an $\text{AME}(n, d)$ state has minimal support if it can be written as a linear combination of $d^{\lfloor n/2 \rfloor}$ fully separable orthogonal pure states. Here, we consider superposition at the level of vectors, in such a way that the linear combination of pure states always produce another pure state. For example, generalized Bell states for two-qudit systems and generalized GHZ states for three-qudit systems have minimal support. It is simple to show that all coefficients of every AME state having minimal support can be chosen to be identically equal to $d^{-\lfloor n/2 \rfloor/2}$, that is, identical positive numbers. By contrast, AME states having non-minimal support will need non-trivial phases to have all reduced density matrices proportional to the identity. In other words, non minimal support AME states require destructive interference.

Furthermore, AME states connect to different mathematical ideas. It is known that AME states having minimal support, e.g. $\text{AME}(2,2)$, $\text{AME}(3,2)$ and $\text{AME}(4,3)$, are one-to-one related to a special class of maximum distance separable (MDS) codes [24], index unity orthogonal arrays [25], permutation multi-unitary matrices when n is even [15] and to a set of $m = n - \lfloor n/2 \rfloor$ mutually orthogonal Latin hypercubes of size d defined in dimension $\lfloor n/2 \rfloor$ [26]. On the other hand, AME states inequivalent to minimal support states, e.g. $\text{AME}(5,2)$ or $\text{AME}(6,2)$, are equivalent to quantum error correction codes [20], quantum orthogonal arrays [26], non-permutation multiunitary matrices [15] and $m = N - \lfloor n/2 \rfloor$ mutually orthogonal quantum Latin hypercubes of size d defined in dimension $\lfloor n/2 \rfloor$ [26].

AME states define an interesting mathematical problem itself but also they define attractive practical applications. These include quantum secret sharing [16, 18], open destination quantum teleportation [18] and quantum error correcting codes [20], the last one being a fundamental ingredient for building a quantum computer.

B. Explicit expressions of AME states

Let us present the explicit expressions of the more fundamental, yet non-trivial AME states.

The first examples are related to qubits. It can be seen very easily that GHZ states for $n = 2$ and $n = 3$ give raise to reduced density matrices which are proportional to the identity. This is sort of trivial as for two qubits there is only one partition, and for three qubits one of them is a simple qubit. It is not obvious to find that there are no AME states for $n = 4$ qubits [22]. The interesting results occur for $n = 5$ [27] and $n = 6$ [28]. The AME(5,2) state can be written as

$$|\Upsilon_{5,2}\rangle = \frac{1}{4\sqrt{2}} \sum_{i=1}^{32} c_i |i\rangle, \quad (1)$$

where we use the standard short-hand notation for the computational basis and where

$$c_i = \{1, 1, 1, 1, 1, -1, -1, 1, 1, -1, -1, 1, 1, 1, 1, 1, -1, -1, 1, -1, 1, -1, -1, 1, -1, -1, 1, 1, 1\}. \quad (2)$$

Using local unitary operations, the same state can be reduced to any of the following states [16, 29],

$$\begin{aligned} |0_{L1}\rangle &= \frac{1}{4} (|00000\rangle + |10010\rangle + |01001\rangle + |10100\rangle + |01010\rangle - |11011\rangle - |00110\rangle - |11000\rangle \\ &\quad - |11101\rangle - |00011\rangle - |11110\rangle - |01111\rangle - |10001\rangle - |01100\rangle - |10111\rangle + |00101\rangle), \\ |1_{L1}\rangle &= \frac{1}{4} (|11111\rangle + |01101\rangle + |10110\rangle + |01011\rangle + |10101\rangle - |00100\rangle - |11001\rangle - |00111\rangle \\ &\quad - |00010\rangle - |11100\rangle - |00001\rangle - |10000\rangle - |01110\rangle - |10011\rangle - |01000\rangle + |11010\rangle). \end{aligned} \quad (3)$$

For $n = 6$, an AME(6,2) state can be constructed from the above AME(5,2) states $|0_{L1}\rangle$ and $|1_{L1}\rangle$ as

$$\begin{aligned} |\Omega_{6,2}\rangle &= \frac{1}{\sqrt{2}} (|0\rangle |0_{L1}\rangle + |1\rangle |1_{L1}\rangle) \\ &= \frac{1}{4} [|000\rangle (|+-+\rangle + |-+-\rangle) - |001\rangle (|+-\rangle - |-+\rangle) + |010\rangle (|+-\rangle - |--\rangle) \\ &\quad - |011\rangle (|+++ \rangle + |--\rangle) - |100\rangle (|+++ \rangle - |--\rangle) - |101\rangle (|+-\rangle + |--\rangle) \\ &\quad - |110\rangle (|+-\rangle + |-+\rangle) - |111\rangle (|+-\rangle - |-+\rangle)], \end{aligned} \quad (4)$$

where $|\pm\rangle = (|0\rangle \pm |1\rangle) / \sqrt{2}$. This exemplifies that local unitaries can be used to find versions of an AME state with a reduced support. Similarly, an AME(5,2) state having eight real coefficients can be found by combining the two states

$$|0_{L2}\rangle = \frac{1}{2} (|00000\rangle + |00011\rangle + |01100\rangle - |01111\rangle), \quad (5)$$

$$|1_{L2}\rangle = \frac{1}{2} (|11010\rangle + |11001\rangle + |10110\rangle - |10101\rangle) \quad (6)$$

in the following way [15]:

$$|\Omega_{5,2}\rangle = \frac{1}{\sqrt{2}} (|0_{L2}\rangle + |1_{L2}\rangle). \quad (7)$$

Yet, neither the five- nor six-qubit AME states have minimal support.

To allow perfect reductions of the reduced density matrices with minimal support states, the dimension of the local Hilbert space has to be larger than two. This is the case of AME(4,3), that can be written as

$$\begin{aligned} |\Omega_{4,3}\rangle &= \frac{1}{3} \sum_{i,j=0}^2 |i\rangle |j\rangle |i+j\rangle |i+2j\rangle \\ &= \frac{1}{3} (|0000\rangle + |0111\rangle + |0222\rangle + |1012\rangle + |1120\rangle + |1201\rangle + |2021\rangle + |2102\rangle + |2210\rangle). \end{aligned} \quad (8)$$

In a similar way, we can derive the AME(6,4) state [25]:

$$\begin{aligned}
|\Omega_{6,4}\rangle = \frac{1}{8} & (|000000\rangle + |111100\rangle + |222200\rangle + |333300\rangle + |321010\rangle + |230110\rangle + |103210\rangle + |012310\rangle \\
& + |132020\rangle + |023120\rangle + |310220\rangle + |201320\rangle + |213030\rangle + |302130\rangle + |031230\rangle + |120330\rangle \\
& + |231001\rangle + |320101\rangle + |013201\rangle + |102301\rangle + |110011\rangle + |001111\rangle + |332211\rangle + |223311\rangle \\
& + |303021\rangle + |212121\rangle + |121221\rangle + |030321\rangle + |022031\rangle + |133131\rangle + |200231\rangle + |311331\rangle \\
& + |312002\rangle + |203102\rangle + |130202\rangle + |021302\rangle + |033012\rangle + |122112\rangle + |211212\rangle + |300312\rangle \\
& + |220022\rangle + |331122\rangle + |002222\rangle + |113322\rangle + |101032\rangle + |010132\rangle + |323232\rangle + |232332\rangle \\
& + |123003\rangle + |032103\rangle + |301203\rangle + |210303\rangle + |202013\rangle + |313113\rangle + |020213\rangle + |131313\rangle \\
& + |011023\rangle + |100123\rangle + |233223\rangle + |322323\rangle + |330033\rangle + |221133\rangle + |112233\rangle + |003333\rangle). \quad (9)
\end{aligned}$$

This state is formed by $4^3 = 64$ equally superposed orthogonal states, so it is an AME state of minimal support.

III. QUANTUM CIRCUITS TO CONSTRUCT AME STATES

As mentioned above, AME states can be constructed in different ways. For our propose, the graph state formalism is the most convenient one [30]. Graph states are represented by a graph, where each vertex corresponds to a $|+\rangle$ state – that is, the superposition of all one-qudit states of the computational basis – and each edge with a CZ gate. We can easily construct the quantum circuit from the graph by considering a simple rule. In addition, a graph can be transformed into another -equivalent one- by applying local unitary operations [31]. This kind of transformation modifies the number of edges of a graph but not its entanglement properties. This property allows us to adapt each circuit to different quantum chip architectures in order to reduce as much as possible the number of gates required to physically implement the states.

Graph states can be defined in any local dimension d . However, most current quantum computers can only implement qubit quantum circuits which forbids the possibility of generating AME states of greater dimension or involving more parties in current devices. We can try to avoid this inconvenience by simulating AME states of grater dimension using qubits, that is, by mapping each qudit state into a multi-qubit state and by adapting the d -dimensional gates operations into this map.

A. Graph States

Graph states are a type of pure quantum states that can be constructed from a graph formed by $\mathcal{V} = \{v_i\}$ vertices and connected by $\mathcal{E} = \{e_{ij} = \{v_i, v_j\}\}$ edges. Each graph has a corresponding adjacency matrix \mathcal{A} , whose entries A_{ij} provide the weights of each edge e_{ij} . An entry A_{ij} vanishes if and only if vertices i and j are disconnected. Also, in graph states self-interactions are forbidden, meaning that diagonal entries of A vanish. A graph state for n qudits can be constructed as follows [30]:

$$|G\rangle = \prod_{i<j}^n \text{CZ}_{ij}^{A_{ij}} (F_d|\bar{0}\rangle)^{\otimes n}, \quad (10)$$

where

$$\text{CZ}_{ij} = \sum_{k=0}^{d-1} \omega^{kl} |\bar{k}\rangle\langle\bar{k}|_i \otimes |\bar{l}\rangle\langle\bar{l}|_j, \quad (11)$$

is the generalized controlled- Z gate, $\omega = e^{2\pi i/d}$ and

$$F_d = \frac{1}{\sqrt{d}} \sum_{k=0}^{d-1} \omega^{kl} |\bar{k}\rangle\langle\bar{l}|, \quad (12)$$

is the Fourier qudit gate. From now on, to distinguish between qubits and qudits states, we will write a bar on qudit states and keep the usual notation, with no bar, for qubits.

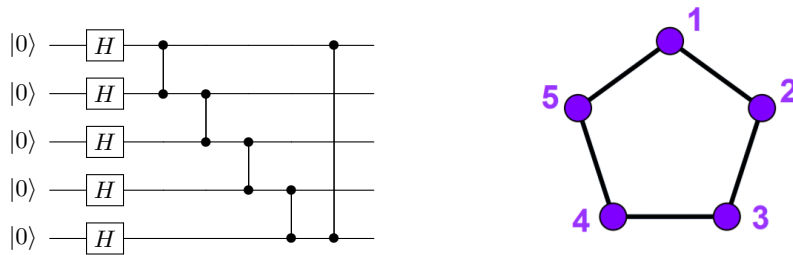


Figure 1: Quantum circuit to generate AME(5,2) and its corresponding graph.

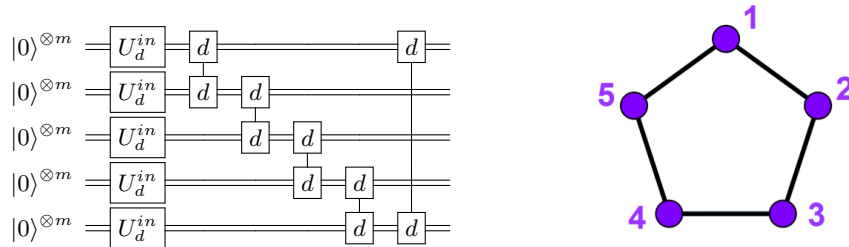


Figure 2: Graph state (right) that generates an AME(5,d) state and its corresponding circuit (left) by using qubits instead of qudits. The number of qubits needed to represent each qudit is $m = \lceil \log_2 d \rceil$. First, qubits are prepared in the basis superposition state by using U_d^{in} , which corresponds to H for qubits, U_3^{in} of Figure 6 for qutrits and $U_4^{in} = H \otimes H$ for ququarts. Then, CZ gates are performed between the qudits, which for $d = 3$ and $d = 4$ can be implemented with the circuit shown in Figures 7 and 8, respectively.

Following the above definition, the explicit construction of a graph state from its corresponding graph is straightforward. First, each vertex corresponds with the qudit state $|\psi_0\rangle = F_d|\bar{0}\rangle$, and second, each edge corresponds with a CZ gate applied between two vertices. For instance, consider the quantum circuit generating the AME(5,2) state, see Figure 1. For qubits, note that F_2 gate is actually the Hadamard gate. Preparation of a qubit graph state (10) is equivalent to initialize all qubits in the state $|+\rangle = (|0\rangle + |1\rangle)/\sqrt{2}$ and then apply CZ gates between the qubits according to the chosen graph.

Notice that after applying the Fourier gates F_d we obtain a state with all basis elements. Then, since the CZ gates only introduce relative phases between these elements, the final state of a graph contains a superposition of the d^n elements of the computational basis.

Graph states can also be described by using stabilizer states [32]. They find application in quantum error correcting codes [33] and one-way quantum computing [34]. A graphical interpretation of entanglement in graph states is provided in Ref.[35] and multipartite entanglement properties in qubit graph states, as well as its optimal state preparation, has been studied in Ref. [30, 36, 37].

B. AME states from graph states

We can write an AME state by using its corresponding graph, as described above. This is a particular form of an AME state having maximal support, as we have the superposition of all elements of the computational basis.

We will be interested in finding the optimal AME graph states, i.e. those graphs with minimum number of edges and coloring index [36]. The smaller the number of edges the smaller the number of operations required to generate AME states. Coloring index is related with the number of operations that can be performed in parallel, so it is proportional to the circuit depth.

Finding new AME graph states is a hard task, as we increase the local dimension d and the number of parties n . Fortunately, there are some suitable tools useful to simplify the construction of graphs for specific values of d and n [35].

The first interesting property is that some graph states can be constructed in any dimension d . The former examples are the Bell and GHZ states, the AME states of $n = 2$ and $n = 3$ parties, respectively, in any dimension d . The graph states of $n = 5$ and $n = 6$, shown in Figures 2 and 3 respectively, work for any prime dimension d . The $n = 4$ graph state of Figure 4 also fulfills this property but for prime dimension $d \geq 3$.

For a non-prime local dimension there exist some methods to find AME graph states [35]. One of those consists

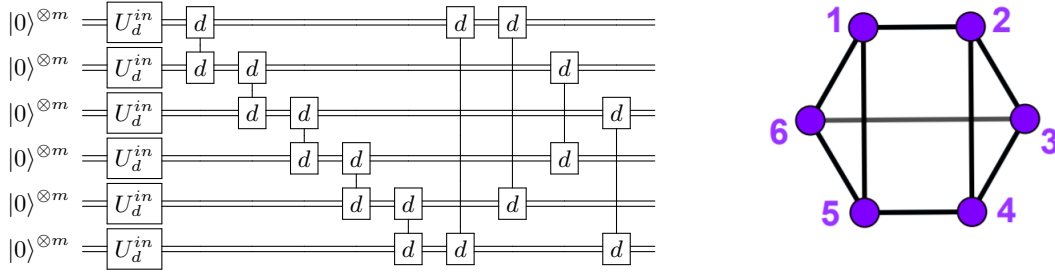


Figure 3: Graph state (right) that generates an $\text{AME}(6,d)$ state and its corresponding circuit (left) by using qubits instead of qudits. The number of qubits needed for represent each qudit is $m = \lceil \log_2 d \rceil$. Qubits are prepared by using U_d^{in} and CZ gates in dimension d , simulated by using the circuits shown in Figures 7 and 8.

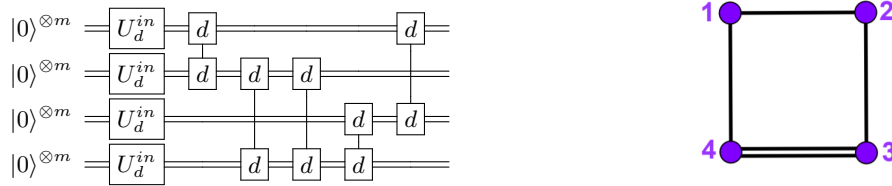


Figure 4: Graph state (right) that generates an $\text{AME}(4,d)$ state for any prime dimension $d \geq 3$ and its corresponding circuit (left) by using qubits instead of qudits.

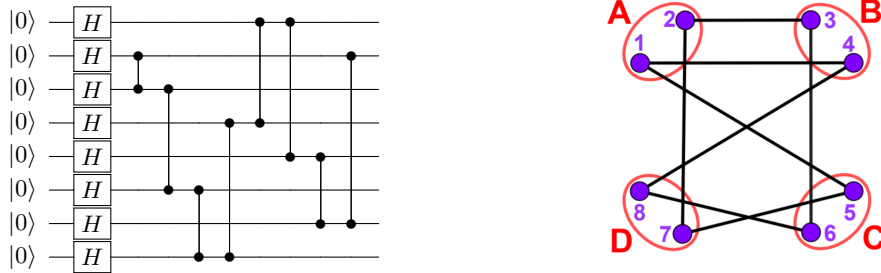


Figure 5: Quantum circuit producing the $\text{AME}(4,4)$ state with qubits (left) and its corresponding graph (right). Parties A , B , C and D are maximally entangled between them but not the qubits inside each party. Notice that this circuit does not correspond to an $\text{AME}(8,2)$ state, since this AME state does not exist.

on taking the prime factorization $d = d_1 d_2 \cdots d_m$ and look for the $\text{AME}(n, d_i)$ states independently. If they exist, the $\text{AME}(n, d)$ is just the tensor product of the $\text{AME}(n, d_i)$ states. In case prime factorization of d includes a power of some factor, we can construct an AME state by artificially defining each party, i.e. by using qudits in lower dimension $m < d$ and then performing the suitable set of CZ gates between the m level qudit systems. For instance, this method has been used to find an the $\text{AME}(4,4)$ state from qubits instead of ququarts (qudits with $d = 4$ levels each), as we illustrate in Figure 5. The -real- local dimension of each party, $d = 4$, is achieved by grouping qubits in pairs [35].

C. AME states circuits using qubits

Figures 2–5 and Bell and GHZ states serve to construct $\text{AME}(2,d)$, $\text{AME}(3,d)$, $\text{AME}(5,d)$, $\text{AME}(6,d)$, $\text{AME}(4,d)$ and $\text{AME}(4,4)$ states with $d \geq 3$, whenever d is a prime number. Moreover, we can use a combination of these graphs to construct AME states of greater d , as it has been explained in the previous subsection.

The construction of a qubit quantum circuit from a graph state is straightforward since we just have to perform Hadamard gates on all qubits initialized at $|0\rangle$ state and CZ gates, according to graph edges. These quantum gates are commonly used in current quantum devices, e.g. in quantum computing [38]. However, if we are interested in generating an AME state of $d > 2$ we may need a qudit quantum computer that can perform quantum operations beyond binary quantum computation. The construction of such device is much more challenging than the current

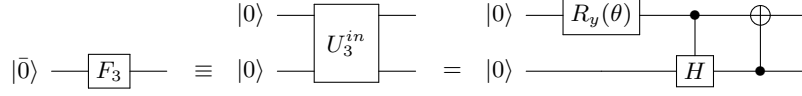


Figure 6: Quantum circuit to obtain $|\bar{\psi}_0\rangle$ qutrit state using two qubits, i.e. to generate $|\psi_0\rangle = (|00\rangle + |01\rangle + |10\rangle)/\sqrt{3}$ state. The angle of the rotational gate is $\theta = -2 \arccos(1/\sqrt{3})$.

quantum computers and, therefore, perform such kind of experiment become really hard. For that reason, we propose to simulate these AME states having greater local dimension by using qubits instead of qudits. To do so, we translate the local dimensions d into multiqubit states. For instance, to transform a ququart system $d = 4$ into a two qubit system $m = 2$ we consider the following identification

$$|\bar{0}\rangle \equiv |00\rangle, \quad |\bar{1}\rangle \equiv |01\rangle, \quad |\bar{2}\rangle \equiv |10\rangle, \quad |\bar{3}\rangle \equiv |11\rangle. \quad (13)$$

For $d > 4$, we need to increase the number of qubits accordingly, i.e. we need $m = \lceil \log_2 d \rceil$ qubits to describe each d -level system. Since we have the graphs for these states, the challenge is to simulate the effect of the generalized CZ gate (11) and the Fourier gate (12), with qubit gates. To be precise, we are not interested in the exact Fourier gate but on generating the state $|\bar{\psi}_0\rangle = F_d|\bar{0}\rangle$. For that propose, we will look for an initialization gate U_d^{in} that acts on qubits in the state $|0\rangle$ and obtains the $|\psi_0\rangle$ state, i.e. the state $|\bar{\psi}_0\rangle$ written in terms of qubits according to the mapping of Eq.(13).

When d is a power of 2, the state $|\bar{\psi}_0\rangle$ can be generated easily using only Hadamard gates. In particular, for $d = 4$ we have

$$|\bar{\psi}_0\rangle = F_4|\bar{0}\rangle = \frac{1}{2} (|\bar{0}\rangle + |\bar{1}\rangle + |\bar{2}\rangle + |\bar{3}\rangle) \rightarrow |\psi_0\rangle = U_4^{in}|00\rangle = (H \otimes H)|00\rangle = \frac{1}{2} (|00\rangle + |01\rangle + |10\rangle + |11\rangle). \quad (14)$$

Despite $F_4 \neq U_4^{in} = (H \otimes H)$, we consider the tensor product unitary transformation, as we just want to obtain the state $|\bar{\psi}_0\rangle$ with qubits.

For $d = 3$ the state $|\bar{\psi}_0\rangle$ can be obtained from the gate U_3^{in} , defined in Figure 6:

$$|\bar{\psi}_0\rangle = F_3|\bar{0}\rangle = \frac{1}{\sqrt{3}} (|\bar{0}\rangle + |\bar{1}\rangle + |\bar{2}\rangle) \rightarrow |\psi_0\rangle = U_3^{in}|00\rangle = \frac{1}{\sqrt{3}} (|00\rangle + |01\rangle + |10\rangle). \quad (15)$$

In general, the circuit producing the state $|\psi_0\rangle$ is hard to find, except when d is a power of 2, as explained above. On the contrary, a circuit implementing the generalized CZ gate is simpler since this gate only introduces a phase in some qudit states and we can reproduce this effect by using controlled-Phase gates, i.e. $CPh(\theta) = |00\rangle\langle 00| + |01\rangle\langle 01| + |10\rangle\langle 10| + e^{i\theta}|11\rangle\langle 11|$.

Figure 7 shows the required circuit to implement generalized CZ gate for qutrits with qubits. We need four qubits and four CPh gates to achieve the expected result of this gate. The quantum circuit required to implement the generalized CZ gate for ququarts is shown in Figure 8. Only three gates are needed here: two qubit CZ gates and a controlled-S gate, which is a CPh with $\theta = \pi/2$.

At this point, all ingredients to construct the AME states for qubits and to simulate AME states with local dimension $d > 2$ has been introduced. Figures 2 and 3 can be used to simulate any AME(5, d) and AME(6, d) state with qubits, providing U_d^{in} and CZ gates. Similarly, Figure 4 can be used to simulate any AME(4, d) state for prime dimension $d \geq 3$. Finally, Figure 5 shows explicitly the circuit and the graph required to obtain the AME(4,4) state.

D. AME states circuits of minimal support

Since AME states of minimal support have connections with error correcting codes, it could be interesting to find the corresponding quantum circuits to generate them.

For qutrits, the AME(4,3) state of Eq.(8) has minimal support. The quantum circuit that generates this state is shown in Figure 9 [15]. The quantum gates required to construct this circuit are the Fourier transform gate for qutrits F_3 and the C_3 -adder gate

$$\bar{C}_3|i\rangle|j\rangle = |i\rangle|\overline{i+j}\rangle, \quad (16)$$

which is the generalization of CNOT gate for qutrits. It is represented with the CNOT symbol with the superscript 3, see Figure 9.

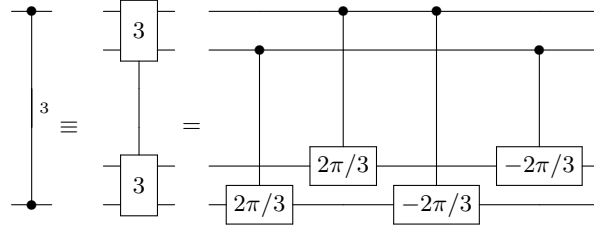


Figure 7: Generalized CZ gate for qutrits, $d = 3$, performed with four qubits. First two CPh gates and last two CPh gates can be implemented in parallel, so the circuit depth is just 2 CPh gates.

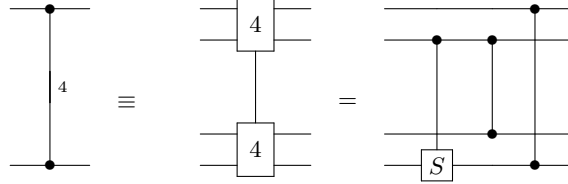


Figure 8: Generalized CZ gate for ququarts, $d = 4$, performed with four qubits. First gate is a controlled-S gate, which is actually a CPh gate with $\theta = \pi/2$. Last two CZ gates can be implemented in parallel, so the circuit depth is just 2 gates.

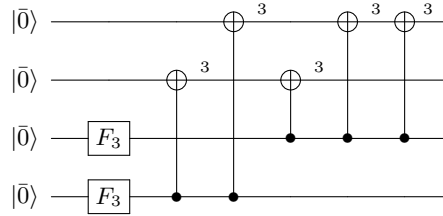


Figure 9: Quantum circuit required to generate the state $|\Omega_{4,3}\rangle$ (4 qutrits) based on the Fourier gate F_3 and C_3 -adder gate for qutrits.

The simulation of the state $F_3|\bar{0}\rangle$ by using qubits has been already explained in the previous subsection. The construction of the C_3 -adder gate is more cumbersome and we leave the details to the Appendix A. The strategy that we use consists in using controlled gates that allow us to perform the sums separately for each control state. If the control qutrit is in the state $|\bar{0}\rangle$ we should apply the identity, so that no gates are needed in this case. If the control qutrit is prepared in the state $|\bar{1}\rangle$, i.e. $|01\rangle$, then we should implement CNOT and Toffoli gates (CCNOT) that take the second qubit as a control qubit, i.e. the second pair of qubits is not affected when the first two are prepared in a different state. Similarly, if the qutrit state is $|\bar{2}\rangle$, i.e. $|10\rangle$, we should search for a sequence of CNOT and CCNOT gates that implement the corresponding sums by using as a control qubit the first qubit.

The resulting circuit is depicted in Figure 10, where we have used approximate CCNOT gates described in Figure 11, CCNOT_a and CCNOT_b , instead of usual CCNOT gates in order to reduce significantly the circuit depth [39]. This circuit is divided in two sectors, each one performing the C_3 -adder gate if the controlled qubit is $|\bar{1}\rangle$, the first 3 gates, or $|\bar{2}\rangle$, the last 3 gates. Any of those gates affect the qubit state if the control qutrit is in the $|\bar{0}\rangle$ state.

Clearly, the C_3 gate is the responsible for the growth of circuit depth. However, we can implement the first two adders by using two CNOT gates each one taking advantage that the target qutrit state is $|\bar{0}\rangle$, i.e. qubits are prepared in the state $|00\rangle$.

The final circuit to simulate the state $|\Omega_{4,3}\rangle$ by using two qubits to represent each qutrit is shown in Figure 12, where CZ gates are framed because they are only necessary if we are implementing the CCNOT_a .

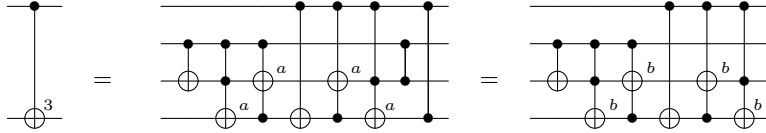


Figure 10: C_3 -adder implemented with approximate Toffoli gates of Figure 11. The C_3 -adder that uses the $CCNOT_a$ gates needs extra controlled-Z gates to cancel out the minus signs introduced by the approximation.

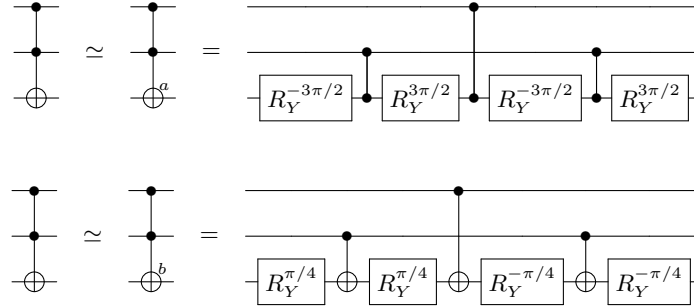


Figure 11: Approximations of CCNOT gate. They introduce a change of sign in some states, in particular $CCNOT_a|101\rangle = -|101\rangle$ and $CCNOT_b|100\rangle = -|100\rangle$.

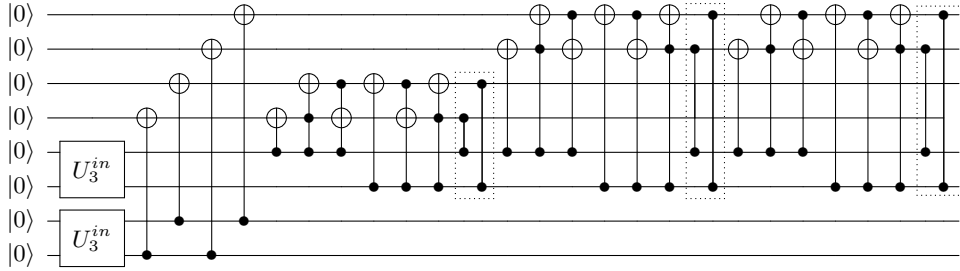


Figure 12: Circuit for the construction of the AME(4,3) state by using two qubits to represent each qutrit. The controlled-Z gates (framed with dots), are only necessary when we use the approximation of Toffoli gate $CCNOT_a$.

IV. ENTANGLEMENT MAJORIZATION

Majorization has deep implications in quantum information theory [40]. In particular, quantum algorithms obey a majorization arrow, which means that majorization could be at the core of their efficiency [41, 42]. Following this idea, we wonder whether the above quantum circuits obey majorization. If not, it is interesting to asking whether more efficient circuits obeying majorization exist.

Let $\mathbf{a}, \mathbf{b} \in \mathbb{R}^d$ be vectors having entries ordered in decreasing order, namely \mathbf{a}^\downarrow and \mathbf{b}^\downarrow with $a_{i+1}^\downarrow \geq a_i^\downarrow$, and similarly for \mathbf{b}^\downarrow . We say that \mathbf{a} majorizes \mathbf{b} , i.e. $\mathbf{a} \succ \mathbf{b}$, iff

$$\sum_{i=1}^k a_i^\downarrow \geq \sum_{i=1}^k b_i^\downarrow \quad \text{for } k = 1, \dots, d, \quad (17)$$

and $\sum_{i=1}^d a_i = \sum_{i=1}^d b_i$.

First, we should choose a set of parameters to study if they majorize at each step during the computation, i.e. after the application of each CZ gate. Since all circuits start with a product state and finish with a maximally entangled state in all bipartitions, a natural choice will be the eigenvalues of the reduce density matrices. At some step s during the computation, the circuit has generated a quantum state with density matrix ρ_s . We then compute the reduce

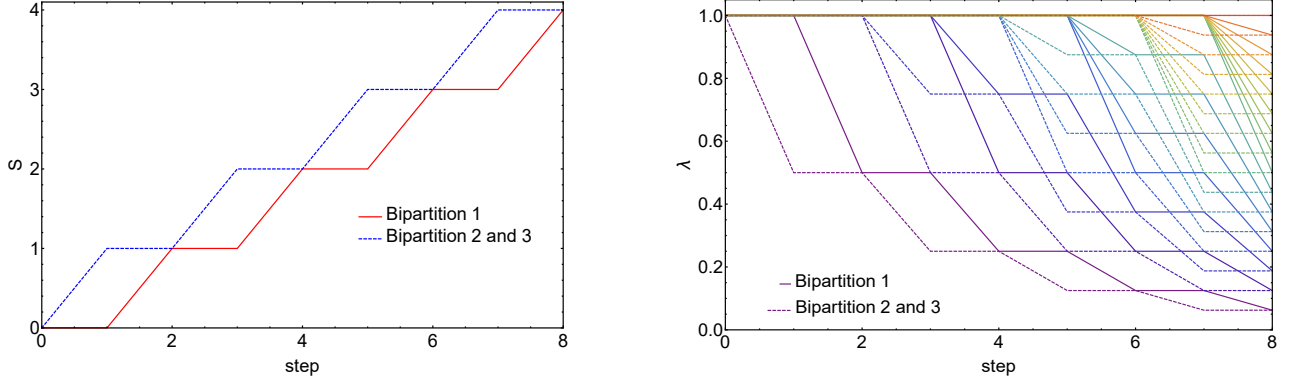


Figure 13: Majorization in AME(4,4) state circuit of Figure 5. Left: entropy increases at each step s in all bipartitions until it reach the maximum value $S = 2 \log_2 4 = 4$. Right: majorization in terms of eigenvalues of the reduce density matrix. At the end of the computation, all eigenvalues are the same, which leads to a density matrix proportional to the identity.

density matrix of every of its bipartitions in two subsystems, A and B , i.e. $\rho_A^s = \text{Tr}_B \rho_s$, and diagonalize this matrix to obtain its eigenvalues $\lambda^s = \{\lambda_i^s\}$. We will establish that this circuit obeys majorization iff $\lambda^s \succ \lambda^{s+1}$, i.e.

$$\sum_{i=1}^k \left(\lambda_i^s\right)^s \geq \sum_{i=1}^k \left(\lambda_i^{s+1}\right)^{s+1} \quad \text{for } k = 1, \dots, d^m - 1 \quad \forall A, s, \quad (18)$$

where $m = n - \lfloor n/2 \rfloor$ is the number of qudits in A bipartition. We do not consider last summation $k = d^m$ because the eigenvalues of a density matrix are normalized to the unity. Since there are $\binom{n}{\lfloor n/2 \rfloor}$ bipartitions, this analysis leads to a total number of $\binom{n}{\lfloor n/2 \rfloor} (d^m - 1)$ inequalities to fulfil.

We can apply less strict tests if we just look at the majorization of other figures of merit to quantify bipartite entanglement, for instance Von Neumann entropy or purity, which in terms of λ_i are defined as $S = -\sum_i \lambda_i \log_d \lambda_i$ and $\gamma = \sum_i \lambda_i^2$ respectively. Both functions in terms of λ_i are convex, so we can apply the Karamata's inequality [43] to prove that

$$\begin{aligned} \lambda^s \succ \lambda^{s+1} &\Rightarrow S^s \leq S^{s+1} \\ &\Rightarrow \gamma^s \geq \gamma^{s+1}. \end{aligned} \quad (19)$$

See Appendix ?? for further details. Thus, we can first do one of these less restrictively tests and if the above inequalities are not fulfilled in all steps, then we can conclude that there is no majorization in eigenvalues.

As an example, Figure 13 shows the majorization of AME(4,4) state of Figure 5 in terms of entropy and eigenvalues of the reduce density matrix for each bipartition. The circuit majorizes since entropy never decreases and eigenvalues never increase at each step. At the end of the computation, all bipartition have reached the maximum value $S = 2 \log_2 4 = 4$ when all eigenvalues are identical, meaning that reduced density matrices are proportional to the identity, as expected for an AME state.

After analyzing the circuit to construct the state $|\Omega_{4,3}\rangle$ written in Figure 9, we found that it do not majorize, i.e. when the fourth C_3 -adder is applied, the entropy of one of the bipartitions decreases before reaching the maximum value after the application of the last C_3 -adder gate. For this reason, we conclude that this circuit is not optimal, being possible to obtain an AME(4,3) state with minimal support from a smaller number of gates. In particular, we found many equivalent circuits that can obtain this kind of state with only four C_3 -adder gates. An example is shown in Figure 14. Notice that, in this example, two C_3 -adders are applied in parallel, which reduces significantly the circuit depth, specially if we want to simulate this AME with qubits.

We found that all circuits up to $n = 6$ and $d = 4$ majorize except AME(6,2) and AME(6,4). Even in these two cases, only one bipartition does not majorize, which shows the high optimality of the entanglement power of the circuits proposed.

One can use this majorization criteria to find optimal entangling circuits based on graph states. For instance, if we are interested in entangle eight parties of our circuit, we can construct a greedy algorithm that finds such a circuit by imposing entanglement majorization. Moreover, we can restrict this algorithm to the given chip architecture, making it suitable for the experimental implementation.

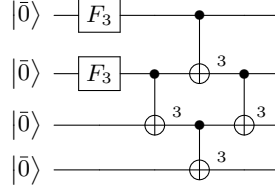


Figure 14: Quantum circuit to obtain an AME(4,3) of minimal support. This circuit has been found after applying a majorization test in circuit of Figure 9. The number of C_3 -adder gates and circuit depth have been reduced in one unit, since two of these gates can be applied in parallel. For the qubit simulation, this is a significant gain in terms of circuit complexity.

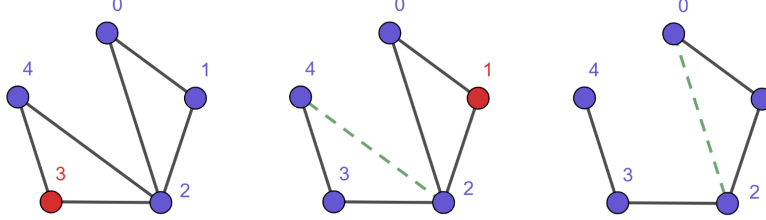


Figure 15: Left graph shows the `ibmqx4` connectivity. After applying LU operations, one can transform this graph into the linear graph, which belongs to a different graph state class than the one that includes the AME state [30]. The recipe is the following: taking one vertex (in red), one connects all vertices that are connected with the selected one or, in case they are connected, one erase these edges (dashed green lines). This result means that more connections are necessary in order to generate the AME(5,2) graph state in this device.

V. EXPERIMENTAL IMPLEMENTATION

The experimental implementation of an AME state requires the use of some figure of merit to certify the generation of such state. For qubit AME states of $n = 2$ and $n = 3$ one can use the computation of a Bell inequality, since Bell and GHZ states (which are an AME(2,2) and an AME(3,2) respectively) violate maximally these inequalities [13]. For AME(5,2), AME(6,2) and other graph states, there exist a family of Bell inequalities that are maximally violated by these states [44]. Besides Bell inequalities, one can implement a quantum tomography protocol to reconstruct the AME state, being the fidelity of state reconstruction the figure of merit. This kind of protocols require a quadratic number of measurements outcomes, as a function of the dimension of the Hilbert space [45–47]. However, this number can be reduced to scale linearly when *a priori* information about the state is available, e.g. nearly pure quantum state [48].

Regardless which protocol is more convenient to implement the AME state test, we have run some AME state circuits in current quantum computers and have check if the probabilities obtained for each basis element are consistent with the AME state probabilities. This is not a final test, since AME states require specific phases between the orthogonal states that cause the necessary cancellations in the reduce density matrices. However, this could provide a first approximation to the expected results.

We have run two circuits to generate an AME(5,2) state in two quantum computers: the `ibmqx4` device from IBM company [49] and the Acorn device from Rigetti computing [50]. Due to qubits connectivity, it would not be always possible to implement the more optimal graph states. For instance, the `ibmqx4` chip needs from at least one extra CZ gate, as shows Figure 15. For this reason, we looked for a quantum circuit that generates an AME(5,2) state restricting the number of entangling gates to five, like the optimal graph state, and respecting the qubit connectivity. We found such a circuit for `ibmqx4` connectivity although it is not a graph state. This circuit is shown in Figure 16. For the Rigetti device, it was not possible to find any circuit that only uses five entangling gates, so we had to adapt the AME(5,2) graph state to its connectivity by using SWAP gates.

The AME(5,2) state of Figure 16 have the following structure

$$|\text{AME}_{5,2}\rangle = \frac{1}{2\sqrt{2}} (|00000\rangle + |00011\rangle + |01101\rangle + |01110\rangle + |10101\rangle + |10110\rangle + |11000\rangle + |11011\rangle). \quad (20)$$

Thus, the expected probabilities of obtaining each basis elements are $1/8 = 0.125$. The results obtained after running

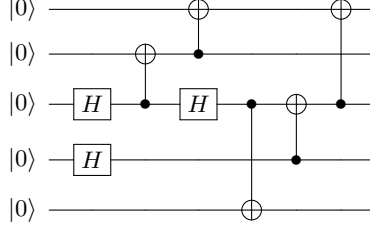


Figure 16: Circuit to generate an AME(5,2) state respecting ibmqx4 device connectivity. Notice that it is not a graph state, since to generate this kind of state one needs more entangling gates.

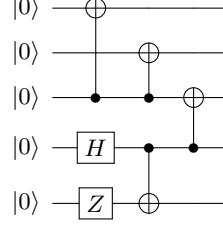


Figure 17: Quantum circuit required to obtain the 5 qubit GHZ state, restricted to the architecture imposed by the 5-qubit IBM quantum computer ibmqx4. It is worth to mention that the experiment has been implemented in December 2017. Nowadays, the restricted architecture of the computer ibmqx4 has been changed.

the circuit of Figure 16 in the ibmqx4 device after 8192 shots were

$$\begin{aligned} |\langle 00000|\psi\rangle|^2 &= 0.105, & |\langle 00011|\psi\rangle|^2 &= 0.058, & |\langle 01101|\psi\rangle|^2 &= 0.038, & |\langle 01110|\psi\rangle|^2 &= 0.128, \\ |\langle 10101|\psi\rangle|^2 &= 0.035, & |\langle 10110|\psi\rangle|^2 &= 0.135, & |\langle 11000|\psi\rangle|^2 &= 0.084, & |\langle 11011|\psi\rangle|^2 &= 0.052, \end{aligned} \quad (21)$$

where $|\psi\rangle$ is the state generated by the quantum device. It seems that only three element basis are correctly generated, $|10110\rangle$, $|01110\rangle$ and $|00000\rangle$. In addition, there appear two computational states among the eighth higher probabilities that are not part of the AME(5,2) state, $|\langle 00010|\psi\rangle|^2 = 0.050$ and $|\langle 00110|\psi\rangle|^2 = 0.042$. These results do not allow us to efficiently implement the tomographic method of Ref. [48], as it requires the correct identification of the zero elements in the computational basis in order to produce a high relative fidelity in state reconstruction.

The results with Acorn chip from Rigetti computing were not distinguishable from noise. Besides the common error sources of the quantum device, the circuit had a greater depth due to the use of SWAP gates.

These results illustrate the difficulty of an AME state test for current quantum computers. Although the circuits are apparently simple and small, the huge amount of entanglement that they generate amplify the effect of the error sources. Additionally, we implemented the GHZ state in the 5-qubit IBM quantum computer ibmqx4, in order to test violation of the 5-qubit Mermin Bell inequality

$$\begin{aligned} M_5 = & -(a_1 a_2 a_3 a_4 a_5) + (a_1 a_2 a_3 a'_4 a'_5 + a_1 a_2 a'_3 a_4 a'_5 + a_1 a'_2 a_3 a_4 a'_5 + a'_1 a_2 a_3 a_4 a'_5 + a_1 a_2 a'_3 a'_4 a_5 + a_1 a'_2 a_3 a'_4 a_5 \\ & + a'_1 a_2 a_3 a'_4 a_5 + a_1 a'_2 a'_3 a_4 a_5 + a'_1 a_2 a'_3 a_4 a_5 + a'_1 a'_2 a_3 a_4 a_5) - (a_1 a'_2 a'_3 a'_4 a'_5 + a'_1 a_2 a'_3 a'_4 a'_5 + a'_1 a'_2 a_3 a'_4 a'_5 \\ & + a'_1 a'_2 a'_3 a_4 a'_5 + a'_1 a'_2 a'_3 a'_4 a_5), \end{aligned} \quad (22)$$

where a_j and a'_k denote two dichotomic observables for five quantum observers [13]. The state theoretical state achieving the maximal violation of the inequality is the GHZ state, see Figure 17. This inequality has a classical value $C = 4$ and a quantum value $Q = 16$. Optimal settings are given by $a_j = \sigma_x$ and $a'_k = \sigma_y$, for $j, k = 1, 5$. Despite the shortness of the circuit 17, the strong correlation of qubits implies a fast decoherence, which is reflected in a reduction of the strength of violation of the inequality. Indeed, the violation achieved in our experiment achieves 6.90 ± 0.01 , being large enough to confirming the genuine non-local nature of the quantum computer ibmqx4.

VI. DISCUSSION AND CONCLUSIONS

Quantum computing is a challenging field of research quantum mechanics that could change the way we do computations in the future. The ultimate goal of a quantum computer is to coherently control a relatively large number of qubits in such a way that a multipartite quantum protocol can be successfully implemented, despite the inherent decoherence of quantum information. It is naturally to expect that quantum over classical advantage in computing is directly related to the amount of quantum correlations existing in the involved qubits. It is thus a remarkably important task to understand the behaviour of quantum computers when the qubits are prepared in a maximally entangled state.

In this work, we studied the simplest possible ways to implement genuinely multipartite maximally entangled quantum states, so-called absolutely maximally entangled (AME) states, in order to test the strength of quantum correlations in quantum computers. We explicitly showed a collection of quantum circuits required to implement such states in a some simple scenarios composed by a few qubit systems. For higher dimensional Hilbert spaces, where AME states of qubits do not exist, we considered qudit AME states, where every qudit was artificially generated by considering a group of qubits, see Section III. For instance, the lack of the AME state for 8 qubit systems can be supplanted by considering the AME state of 4 ququarts, where every ququart is composed by two qubits. In this way, pairs of qubits are maximally correlated with three complementary pairs of qubits, thus exhibiting a maximal amount of quantum entanglement in a sense, see Figure 5.

One of the main problems when trying to prepare a multipartite quantum circuit over a quantum computer having a restricted architecture is the reduction of the circuit depth. This is so because some bipartite quantum operations –like CNOT– are forbidden for some pairs of qubits, as they cannot communicate directly. This physical limitation considerably extends the length of quantum circuit, as typically one has to consider swap operations to complement the lack of communication. In order to deal with this problem, we designed a tool that finds the optimal quantum circuit to efficiently implement AME states based on entropic majorization of reductions, see Section IV. As an interesting observation, optimal quantum circuits for AME states typically admit monotonically increasing entropies of reductions, implying that those states can be efficiently generated with our algorithm in a few steps, see Figure 13. In other words, our algorithm finds the minimal number of local and non-local quantum gates required to implement those AME states, taking into account the restrictions imposed by the architecture of a realistic quantum chip.

As a further step, we implemented the GHZ state of 5 qubits over a 5-qubit quantum computer provided by IBM, where we optimized the circuit according to the restrictions imposed by the architecture. The figure of merit to quantify the quality of the state preparation was the violation of the 5-qubit Mermin Bell inequality [13], which should be maximally violated for the GHZ state. We achieved the experimental non-local value 6.90 ± 0.01 , where the classical value is $C = 4$ and the quantum value is $Q = 16$. This result demonstrates the genuine non-local nature of the multipartite state, which improves a previously achieved value 4.05 ± 0.06 [10]. These negative results reflect that the current state of the art of the considered quantum computers is not yet ready to fully exploit the strongest quantum correlations existing in 5 and 6 qubit quantum computers. Nonetheless, we remark that some protocols involving a partial amount of multipartite quantum entanglement have been successfully implemented in quantum computers for a few [51, 52] and large [53–55] number of qubits.

Acknowledgements

We specially thank to Felix Huber and Saverio Pascazio for fruitful comments and discussions. ACL and JIL are supported by Project FIS2015-69167-C2-2-P. DG is supported by Grant FONDECYT Iniciación number 11180474 and MINEDUC-UA project, code ANT 1855, Chile. The views expressed are those of the authors and do not reflect the official policy or position of IBM or the IBM Quantum Experience team.

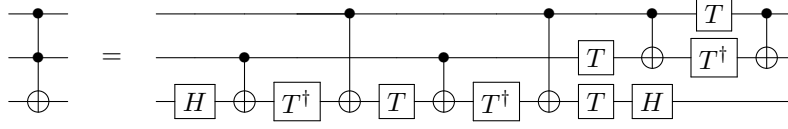
Appendix A: C_3 –adder gate construction

To construct the C_3 –adder gate with qubits we should find a sequence of gates that perform the following operations:

$$\begin{aligned} C_3|00\rangle|00\rangle &= |00\rangle|00\rangle, & C_3|01\rangle|00\rangle &= |01\rangle|01\rangle, & C_3|10\rangle|00\rangle &= |10\rangle|10\rangle \\ C_3|00\rangle|01\rangle &= |00\rangle|01\rangle, & C_3|01\rangle|01\rangle &= |01\rangle|10\rangle, & C_3|10\rangle|01\rangle &= |10\rangle|00\rangle \\ C_3|00\rangle|10\rangle &= |00\rangle|10\rangle, & C_3|01\rangle|10\rangle &= |01\rangle|00\rangle, & C_3|10\rangle|10\rangle &= |10\rangle|01\rangle. \end{aligned} \tag{A1}$$

As a result, besides from CNOT gates, we will need from CCNOT gates. Three-qubit gates are difficult to implement experimentally, so we should decompose them in terms of one and two-qubit gates. The exact decomposition of

CCNOT gate is



which is a circuit of 12 gates of depth. However, we can use instead an approximate decomposition which differ from the previous for some phase shifts of the quantum states other than zero [39]. In particular, we can use the approximate CCNOT gates shown in Figure 11. The only changes that those gates introduce respect the exact CCNOT gate are

$$\text{CCNOT}_a|101\rangle = -|101\rangle, \quad (\text{A2})$$

$$\text{CCNOT}_b|100\rangle = -|100\rangle. \quad (\text{A3})$$

This is translated into the use of controlled-Z gate in the first approximation to obtain the desired result after applying the gate sequence to construct the C_3 -adder. The sign introduced in the CCNOT_b gate is canceled after this sequence, so the circuit remains equal as exact CCNOT gates were used.

We can keep saving more gates. Notice that the firsts two C_3 -adders of the AME circuit of Figure 9 are implemented on qutrits in the state $|\bar{0}\rangle$. Let's write it explicitly. After the Fourier transform on qutrit 1, the circuit applies the C_3 -adder on qutrit 3:

$$(\bar{C}_3)_{13} \left[\frac{1}{\sqrt{3}} (|\bar{0}\rangle + |\bar{1}\rangle + |\bar{2}\rangle)_1 \otimes |\bar{0}\rangle_3 \right] = \frac{1}{\sqrt{3}} (|\bar{0}\bar{0}\rangle + |\bar{1}\bar{1}\rangle + |\bar{2}\bar{2}\rangle)_{13}, \quad (\text{A4})$$

where the subindex 13 stands for the qutrits affected from this operation. In qubits form

$$(C_3)_{13} \left[\frac{1}{\sqrt{3}} (|00\rangle + |01\rangle + |10\rangle)_1 \otimes |00\rangle_3 \right] = \frac{1}{\sqrt{3}} (|00\rangle|00\rangle + |01\rangle|01\rangle + |10\rangle|10\rangle)_{13}. \quad (\text{A5})$$

Then, the above operation consists uniquely in two CNOT gates between even and odd qubits. Similarly, the next C_3 -adder acting on qutrit 4 can be implemented in the same way:

$$(\bar{C}_3)_{14} \otimes \mathbb{I}_3 \left[\frac{1}{\sqrt{3}} (|\bar{0}\bar{0}\rangle + |\bar{1}\bar{1}\rangle + |\bar{2}\bar{2}\rangle)_{13} \otimes |\bar{0}\rangle_4 \right] = \frac{1}{\sqrt{3}} (|\bar{0}\bar{0}\bar{0}\rangle + |\bar{1}\bar{1}\bar{1}\rangle + |\bar{2}\bar{2}\bar{2}\rangle)_{134}, \quad (\text{A6})$$

which in the qubit form becomes

$$(C_3)_{14} \otimes \mathbb{I}_3 \left[\frac{1}{\sqrt{3}} (|00\rangle|00\rangle + |01\rangle|01\rangle + |10\rangle|10\rangle)_{13} \otimes |00\rangle_4 \right] = \frac{1}{\sqrt{3}} (|00\rangle|00\rangle|00\rangle + |01\rangle|01\rangle|01\rangle + |10\rangle|10\rangle|10\rangle)_{134}. \quad (\text{A7})$$

Again, the above state can be obtained from the previous using two CNOT gates, between even and odd qubits. This enormous simplification cannot be extended to the other C_3 -adder gates, as all elements of the basis appear once we implement the F_3 gate on qutrit 2.

-
- [1] E. Magesan, J. M. Gambetta and J. Emerson, *Phys. Rev. A* **85**, 042311 (2012).
 - [2] M. G. A. Paris and J. Reháček, “*Quantum State Estimation*”, Lecture Notes in Physics, Springer-Verlag, Berlin Heidelberg, (2004).
 - [3] S. T. Merkel, J. M. Gambetta, J. A. Smolin, S. Poletto, A. D. Corcoles, B. R. Johnson, C. A. Ryan and M. Steffen, *Phys. Rev. A* **87**, 062119 (2013)
 - [4] R. Blume-Kohout, J. K. Gamble, E. Nielsen, K. Rudinger, J. Mizrahi, K. Fortier and P. Maunz, *Nat. Commun.* **8**, 14485 (2017).
 - [5] D. C. McKay, S. Sheldon, J. A. Smolin, J. M. Chow and J. M. Gambetta, arXiv:1712.06550 [quant-ph] (2017).
 - [6] M. Takita, A. W. Cross, A. D. Corcoles, J. M. Chow and J. M. Gambetta, *Phys. Rev. Lett.* **119**, 180501 (2017).
 - [7] A. W. Cross, L. S. Bishop, S. Sheldon, P. D. Nation and J. M. Gambetta, arXiv:1811.12926 [quant-ph] (2018).
 - [8] R. Blume-Kohout, K. C. Young, arXiv:1904.05546 [quant-ph] (2019).
 - [9] R. Orús, *Ann. Phys. (N. Y.)* **349**, 117 (2014).
 - [10] D. Alsina and J. I. Latorre, *Phys. Rev. A* **94**, 012314 (2016).

- [11] A. Cervera-Lierta, *Quantum* **2**, 114 (2018).
- [12] R. Jozsa and N. Linden, *Proc. R. Soc. London A* **459**, 2011 (2003).
- [13] D. Mermin, *Phys. Rev. Lett.* **65**, 1838 (1990).
- [14] P. Facchi, G. Florio, G. Parisi and S. Pascazio, *Phys. Rev. A* **77**, 060304 (2008).
- [15] D. Goyeneche, D. Alsina, J. I. Latorre, A. Riera and K. Życzkowski, *Phys. Rev. A* **92**, 032316 (2015).
- [16] W. Helwig, W. Cui, A. Riera, J. I. Latorre and H. Lo, *Phys. Rev. A* **86**, 052335 (2012).
- [17] S. Aaronson and A. Arkhipov, *Theory of Computing* **9**, 143 (2013)
- [18] W. Helwig and W. Cui, arXiv:1306.2536 [quant-ph] (2013).
- [19] F. Huber, C. Eltschka, J. Siewert and O. Gühne, *J. Phys. A: Math. Theor.* **51**, 175301 (2018).
- [20] A. J. Scott, *Phys. Rev. A* **69**, 052330 (2004).
- [21] F. Huber, O. Gühne and J. Siewert, *Phys. Rev. Lett.* **118**, 200502 (2017).
- [22] A. Higuchi and A. Sudbery, *Phys. Lett. A* **273**, 213-217 (2000).
- [23] F. Huber, O. Gühne and J. Siewert, *Phys. Rev. Lett.* **118**, 200502 (2017).
- [24] W. C. Huffman and V. Pless, “*Fundamentals of Error-Correcting Codes*”, University Press, Cambridge (2003).
- [25] D. Goyeneche and K. Życzkowski, *Phys. Rev. A* **90**, 022316 (2014).
- [26] D. Goyeneche, Z. Raissi, S. Di Martino and K. Życzkowski, *Phys. Rev. A* **97**, 062326 (2018).
- [27] R. Laflamme, C. Miquel, J. P. Paz and W. H. Zurek, *Phys. Rev. Lett.* **77**, 198 (1996).
- [28] A. Borras, A. R. Plastino, J. Batle, C. Zander, M. Casas and A. Plastino, *J. Phys. A* **40**, 13407 (2007).
- [29] R. Cleve, D. Gottesman and H. Lo *Phys. Rev. Lett.* **83**, 648 (1999).
- [30] M. Hein, J. Eisert and H. J. Briegel, *Phys. Rev. A* **69**, 062311 (2004).
- [31] A. Bouchet, “ *κ -Transformations, Local Complementations and Switching*”, Springer Netherlands, Dordrecht (1990).
- [32] D. Schlingemann, *Quant. Inf. & Comp.* **2**, 307 (2002).
- [33] S. Yong Looi, L. Yu, V. Gheorghiu and R. B. Griffiths, *Phys. Rev. A* **78**, 042303 (2008)
- [34] R. Raussendorf and H. J. Briegel, *Phys. Rev. Lett.* **86**, 5188 (2001).
- [35] W. Helwig, arXiv:1306.2879 [quant-ph] (2013).
- [36] A. Cabello, A. J. López-Tarrida, P. Moreno and J. R. Portillo, *Phys. Lett. A* **373** 2219 (2009).
- [37] A. Cabello, L. E. Danielsen, A. J. Lopez-Tarrida and J. R. Portillo, *Phys. Rev. A* **83** 042314 (2011).
- [38] IBM Quantum Experience, see <https://quantumexperience.ng.bluemix.net>
- [39] A. Barenco, C. H. Bennett, R. Cleve, D. P. DiVincenzo, N. Margolus, P. Shor, T. Sleator, J. Smolin and H. Weinfurter, *Phys. Rev. A* **52**, 3457 (1995).
- [40] M. A. Nielsen and G. Vidal, *Quantum Inf. Compu.* **1**, 76 (2001).
- [41] J. I. Latorre and M. A. Martín-Delgado, *Phys. Rev. A* **66**, 022305 (2002).
- [42] R. Orus, J. I. Latorre, M. A. Martín-Delgado, *Quantum Inf. Process.* **1**, 4, 283–302 (2002).
- [43] Z. Kadelburg, D. Đukić, M. Lukić and I. Matić, *The Teaching of Mathematics* **8**, 31 (2005).
- [44] O. Gühne, G. Tóth, P. Hyllus and H. J. Briegel, *Phys. Rev. Lett.* **95**, 120405 (2005).
- [45] W. K. Wootters and B. D. Fields, *Annals of Physics* **191**, 363–381 (1989).
- [46] J. M. Renes, R. Blume-Kohout, A. J. Scott, and C. M. Caves, *J. Math. Phys.* **45**, 2171–2180 (2004).
- [47] A. J. Scott, *J. Phys. A: Mathematical and General* **39**, 13507–13530 (2006).
- [48] D. Goyeneche, G. Cañas, S. Etcheverry, E. S. Gómez, G. B. Xavier, G. Lima, A. Delgado, *Phys. Rev. Lett.* **115**, 090401 (2015).
- [49] IBM Q team, device specifications <https://github.com/Qiskit/ibmq-device-information/tree/master/backends>.
- [50] J. S. Otterbach *et. al.*, arXiv:1712.05771 [quant-ph].
- [51] S. Debnath, N. M. Linke, C. Figgatt, K. A. Landsman, K. Wright and C. Monroe, *Nature* **536**, 63–66 (2016).
- [52] E. Martinez, C. A. Muschik, P. Schindler, D. Nigg, A. Erhard, M. Heyl, P. Hauke, M. Dalmonte, T. Monz, P. Zoller and R. Blatt, *Nature* **534**, 516 (2016).
- [53] J. Bohnet, B. C. Sawyer, J. W. Britton, M. L. Wall, A. M. Rey, M. Foss-Feig and J. J. Bollinger, *Science* **352**, 6291, 1297 (2016).
- [54] H. Bernien, S. Schwartz, A. Keesling, H. Levine, A. Omran, H. Pichler, S. Choi, A. S. Zibrov, M. Endres, M. Greiner, V. Vuletić and M. D. Lukin, *Nature* **551**, 579–584 (2017).
- [55] J. Zhang, G. Pagano, P. W. Hess, A. Kyprianidis, P. Becker, H. Kaplan, A. V. Gorshkov, Z. X. Gong, C. Monroe, *Nature* **551**, 601 (2017).